Self-consistent-field modeling of hydrated unsaturated lipid bilayers in the liquid-crystal phase and comparison to molecular dynamics simulations

F. A. M. Leermakers
Laboratory of Physical Chemistry and Colloid Science, Wageningen University, Dreijenplein 6, 6703 HB Wageningen, The Netherlands

A. L. Rabinovich
Institute of Biology, Karelian Research Center, Russian Academy of Sciences, Pushkinskaja Street 11, Petrozavodsk 185610, Russia

N. K. Balabaev
Institute of Mathematical Problems of Biology, Russian Academy of Sciences, Pushchino, Moscow Region 142292, Russia
(Received 29 December 2001; published 28 January 2003)

A molecular-level self-consistent-field (SCF) theory is applied to model the lipid bilayer structures composed of 1-stearoyl-2-oleoyl-*sn*-glycero-3-phosphatidylcholine (18:0/18:1ω9*cis* PC) and 1-stearoyl-2-docosahexaenoyl-*sn*-glycero-3-phosphatidylcholine (18:0/22:6ω3*cis* PC). As compared to earlier attempts to model (saturated) PC membranes several additional features are implemented: (i) A water model is used which correctly leads to low water concentration in the bilayers. (ii) Free volume is allowed for, which is important to obtain bilayers in the fluid state. (iii) A polarization term is included in the segment potentials; this new feature corrects for a minor thermodynamic inconsistency present in (all) earlier results for charged bilayers. (iv) The CH_3 groups in the lipid molecules are assumed to have twice the volume of a CH_2 group; this leads to stable noninterdigitated bilayers. (v) A *cis* double bond is simulated by forcing *gauche* conformations along the *sn*-2 acyl chain. Results of an all-atom molecular dynamics (MD) simulation, using the collision dynamics method, on the same system are presented. Both SCF and MD prove, in accordance with experimental facts, that acyl unsaturation effectively reduces the length of the chain which counteracts interdigitation. It is also found that the phosphatidylcholine head group is lying almost flat on the membrane surface and the water penetrates into the bilayer upto the glycerol backbone units. From the SCF results it further followed that the free volume is not exactly evenly distributed over the bilayer. There is a small increase in free volume in the center of the bilayer as well as in the glycerol backbone region.

DOI: 10.1103/PhysRevE.67.011910 PACS number(s): 87.16.Dg, 87.14.Cc, 31.15.Qg, 05.20.−y

INTRODUCTION

Lipid bilayer membranes are amongst the most essential entities of the biological cell. They have fascinating physical and biophysical properties. In this paper the interest is in the structural properties of the bilayer, more specifically, the conformational characteristics of the constituent molecules. It is important to note that all biological cell membranes contain unsaturated phospholipids [1]; in most cases, at least half of the fatty acyl chains of biomembrane lipids are unsaturated. The biological significance of unsaturation in biomembranes is largely recognized (for a review, see Ref. [2]; see also Discussion and outlook section). Nevertheless, it remains unresolved exactly how unsaturation participates in membrane function and/or organization.

Computer aided modeling of lipid bilayer membranes have been used to gain detailed insights (for reviews, see Refs. [3–6]). Several computer simulations of unsaturated and polyunsaturated monolayers and bilayers using molecular dynamics (MD), Monte Carlo and other methods are known [2]. The MD route has been used to obtain both equilibrium structural characteristics as well as short time dynamics. Limitations of MD approach are well known [3–6]: comparatively small number of the particles in the systems studied and/or short simulation time scales (because of time consumption of MD), the parameter choice problem, etc. As a result, phase transitions and various other slow molecular processes are difficult to study by MD. For these reasons there is a need for more coarse grained modeling of the bilayer membrane. Without exceptions these methods are approximate and typically make use of mean-field approximations.

The classical approach to consider the bilayer problem from a mean-field modeling point of view is to model densely packed chains end grafted onto an impenetrable surface [7–15]. In this case it is not necessary to introduce other components than acyl chains. The absence of water is taken as a boundary condition and only the conformational entropy of the tails is considered. Most of these statistical mechanical approaches were not extended to solve the full ''head-and-tails'' problem. The full problem is significantly more complex because not only the head-group properties must be considered, also the water phase and the interactions of the lipid molecules with the water molecules have to be accounted for. The risks for this approach are large. The head-group area is no longer a boundary condition, but must be the result of the calculations. As a consequence, the main parameter is lost to fit the mean-field predictions to experimental and simulation data. A point of historical interest is, that as early as in 1983 the self-consistent-field (SCF) technique was used [16] to show that stable bilayers can be found without the need to graft the lipid tails to a mathematical plane. Around that time the first MD simulations on lipids were still with restricted head groups [17,18]. In line with

experimental findings, it was shown that the *sn*-1 and *sn*-2 tails in, e.g., dimiristoylphosphatidycholine (DMPC) bilayers are not equivalent, the tail closest to the head group is positioned less deep in the bilayer [19]. Another example is the finding that the orientation of the head group in DMPC bilayers is predominantly parallel to the bilayer [20]. It was also shown that it is possible to find the gel-to-liquid phase transition in these bilayers [21]. Another relevant prediction was that phosphatidylcholine (PC) bilayers are only colloid chemically stable at intermediate ionic strength. Both at very low and at very high ionic strength they are attractive [22].

The advantage of the molecular-level SCF modeling is of course that the method can also be used to study properties typically out of reach for MD. For example, the structural properties of lipid vesicles were considered [23]. It was proven recently [26,25,24] that from such an analysis it is possible to obtain unambiguously the Helfrich parameters needed for a mesoscopic analysis of the phase behavior of such systems. It is also straightforward to study bilayers composed of mixtures of different types of amphiphiles or lipid bilayers with additives, etc. Direct comparison to experiments and to related MD simulation proved, however, that it is appropriate to extend the SCF approach once more. In the SCF model used below the following extensions are introduced.

A different model is used to treat the aqueous phase which is similar in spirit to some of the models by Suresh and Naik [27] for associating systems. The water molecules are allowed to cluster in groups of water molecules. The strength by which they can do this is an important parameter in the model. The result of this is that much less water can penetrate into the hydrophobic region of the bilayer. To prevent subsequent crystallization of the bilayer it is necessary to introduce free volume in the calculations. The allowance of free volume also increases the number of parameters in the model. Not only the number of parameters has increased, also the value of the remaining parameters must be adjusted according to the altered properties of the water phase.

To counteract the interdigitation of the acyl tails, it was necessary to consider the CH_3 groups at the end of the lipid tails. In this paper, these groups are modeled having twice the volume of a CH_2 group. In a lattice approach this is realized by a *Y*-type structure at the tail end (chain branching). Again the differentiation between CH_3 and CH_2 groups enables one to express the nonideal mixing of the two components, which may be relevant for the properties of the membrane interior.

As with this refined theory it is possible to model the bilayer membrane more accurately, it is appropriate to attempt a comparison with MD simulations. Of course such comparison can be done on the model lipid DMPC, but it is more challenging to do such comparison for a biologically more interesting case of an unsaturated phosphatidylcholine system. Before this can be attempted, it is necessary to have a strategy how to model double bonds in the lipid tail in a lattice-based SCF approach. Here Cantor [7] is followed. The idea is that the cis double bond is approximately equal to having a forced local *gauche* conformation in the chain. Of course this idea is tested against more accurate implementation of the *cis* double bond in MD simulations.

The remainder of this paper is as follows. Below, details about the SCF model with its extra features are presented. It must be understood that a full discussion of all details of the SCF model cannot be given in this paper; for this we refer to more detailed reports [28]. In the Results section a detailed analysis of the SCF results is presented for liquid-crystalline 1-stearoyl-2-oleoyl-*sn*-glycero-3-phosphatidylcholine (18:0/18:1ω9*cis* PC, SOPC) and 1-stearoyl-2-docosahexaenoyl-*sn*-glycero-3-phosphatidylcholine (18:0/22:6ω3*cis* PC, SDPC) bilayers, see Fig. 2. Below we will use the short-hand notation 18:0/18:1 and 18:0/22:6 for these two lipids, respectively. The key results will be compared to complementary MD data. This enables us to evaluate the status of the SCF modeling. In the final section the insights on the role of lipid unsaturation in membranes will be discussed.

SELF-CONSISTENT-FIELD ANALYSIS

Recently Meijer *et al.* [28] have given a description of the most detailed SCF modeling up to date. This approach will be followed except for basically two points elaborated on below. In order to do this it is necessary to briefly review the basic framework of the SCF model.

The SCF technique can conveniently be split up into two coupled problems. (i) How to find the ensemble averaged conformation distribution, i.e., the segment density profiles, from the segment potentials and (ii) how to find the segment potentials from the segment distributions. For subproblem (i) we follow the procedure of Meijer *et al.* [28] with a single exception for the water molecules. For subproblem (ii) a new term is introduced that accounts for the polarizability of the segments when these are introduced into an electric field. Both problems can be presented once the system and its molecules are discussed.

The discretization scheme and the model for the chains

In principle the (differential) equations that need to be solved in an SCF theory are continuous. Unfortunately, the equations are complex and need to be solved numerically with the aid of a computer. Then it is necessary to discretize the continuous distributions. The result of this operation is usually known by the term ''lattice approximations.'' In the lattice approach the fundamental diffusion equation, which generates the statistical weight of the full set of conformations, transforms into a propagator formalism. The propagator formalism represents a Markov approximation. The consequence of a Markov approximation is that only local along-the-chain excluded-volume correlations are included. For example, in a rotational isomeric state (RIS) scheme, it is possible to guarantee rigorously that the chain is locally nonoverlapping over a distance of four segments. For chain fragments further apart it is not excluded that they occupy the same site. Only through the external potentials a correction for this problem is introduced (see below). In the Markov approximation it is possible to account for the realistic structure of the chain, having semiflexible parts, side chains, etc.

For these details we refer to the literature [28]. Below we will only discuss the formalism in its basic form and omit the propagator formalism.

It is thus necessary to define a discrete set of coordinates onto which segments can be placed. These coordinates are regularly spaced and organized in layers numbered arbitrarily $z=1,2,3,4,\ldots,M$, where the layers 1 and M are the boundary layers in the system. The lattice layers are a distance ℓ apart. Reflecting boundary conditions are imposed, which implies that layer $z=0$ is made identical in all aspects to layer $z=1$ and similarly layer $M+1$ is made identical to layer M. As a consequence a multilamellar system is mimicked, where the membrane-membrane separation is $d=2M\ell$. However, if M is sufficiently large, the effect of nearby membranes is negligible and the results apply for an isolated bilayer. Each lattice layer consists of L sites, where L is taken large enough such that finite size effects are excluded. Each site has an area in the x-y plane of $a=\ell'^2$. In a cubic lattice, which is isotropic, the two length scales are equal, $\ell=\ell'$. In other lattice types, the difference between ℓ and ℓ' corrects for the anisotropy in the lattice. In each layer a mean-field approximation is applied, which effectively means that the lattice sites are indistinguishable. Density gradients are of course allowed in the z direction. The molecules are represented in a united-atom description, where the united atoms are called segments. Segments have a volume equal to one lattice site, i.e., $v_0=\ell(\ell')^2$. The segments in the molecule are linked to each other by bonds. End segments have one, middle segments have two and branch points can have three or four bonds. If the segment is a free monomer it has of course no bonds. The molecule is thus completely defined when the segment types as well as the bonds between segments are specified. The lattice type used in the calculations is the tetrahedral one. In this lattice it is possible to develop a three-choice propagator scheme, wherein the C—C—C—C conformations can "realistically" be represented. In the lattice essentially four bond directions, $\alpha=e,f,g,h$ are distinguished. The directions f and g are two different directions within a layer, e is a direction from layer z to $z-1$, and h is a direction form z to $z+1$. The tetrahedral lattice is anisotropic. This means that a random coil will not automatically be isotropic in this lattice. It is possible, however, to show that when $\ell'=\sqrt{2}\ell$, the chain extends equally far into the x, y, and z directions. Then, $v_o=2\ell^3$.

From segment potentials to segment and bond densities

It follows from the approach of Meijer *et al.* [28] that, in principle, the number of chains in a particular conformation c, where each conformation is defined by the z position of each segment in the chain, is found by

$$n^c = C\prod_{s=1}^{N} G^c(z,s)\prod_{t=1}^{N-1} Z^c_{\alpha_t} G^c(z,\alpha_t) \times \prod_{t=2}^{N-2}\prod_{t>t''\neq t'} \lambda^c(\alpha_{t'},t,\alpha_{t''}), \quad (1)$$

where s is the running parameter over all the segments $s=1,\ldots,N$, t is the index that points to the bonds, $t=1,\ldots,N-1$ (the number of bonds is one less than the number of segments), t' and t'' are also bonds in the molecule and the multiple product with $t>t''\neq t'$ runs over all possible combinations of three consecutive bonds t'—t—t''. The constant C is chosen so as to normalize the distribution, i.e., it fixes the total number of molecules per unit area in the system.

In Eq. (1), $G^c(z,s)$ is the Boltzmann weight that contains the segment potential for segment s in conformation c: $G(z,s)=\exp[-u(z,s)/k_BT]$, where k_BT is the thermal energy. Below it is specified how the segment potentials are found and what contributions should be considered.

The second term in Eq. (1) expresses the weight as a result of placing the bond with ranking number t in the system. It is composed of a factor which corrects for the degeneracy of a conformation: $Z=2$ if the bond direction α of bond t is f or g and $Z=1$ otherwise, and $G^c(z,\alpha_t)$ is an anisotropic weighting factor. This last contribution is linked to the orientation α of the bond t of the molecule. It assumes a high value if the bond is oriented in the same direction as the other bonds in the system near this coordinate and it therefore promotes cooperative orientational transitions. Information on bond orientations is equivalent to knowledge on pairs of sites. Therefore this factor corresponds to a quasichemical approximation for the chain conformations. Indeed by using this ansatz one automatically can reproduce the gel-to-liquid phase transition in the bilayers without the need to invoke extra parameters. Below an expression for $G(z,\alpha_t)$ is given.

The third term in Eq. (1) expresses the statistical weight that originates from the RIS scheme. The term runs over all possible combinations of three neighboring bonds. If t' and t'' are not neighbors of t we have $\lambda=1$ otherwise, when $\alpha_{t'}=\alpha_{t''}$ the local configuration is a trans and the statistical weight is $\lambda_{tr}=1/[1+2\exp[-\Delta U(t)/k_BT]]$ and when this is not the case a *gauche* is present with weight $\lambda_g=(1-\lambda_{tr})/2$. The statistical weight thus is a function of the central bond t. More precisely, $\Delta U(t)$ depends on the segment types of the two segments on both sides of the bond t, i.e., on a sequence of four segments. For a saturated hydrocarbon chain the *trans* configuration is more favorable then the *gauche* conformations. The $\Delta U(t)=U_g(t)-U_{tr}(t)$ is typically positive (order k_BT), except when there is a *cis* double bond. For a *cis* double bond, the local *trans* conformation is made very unfavorable and $\Delta U(\mathrm{C=C})\ll 0$. When t is a bond which takes part of a branch, a value $\Delta U=0$ is implemented. In the lipid molecules there is one asymmetric carbon atom. In the evaluation of the statistical weight of the lipid chain there is no account for chirality and thus it is assumed that a racemic mixture is present.

The overall density distributions $\varphi(z,s)$ for the segments of lipid molecules are found by generating all conformations c with the requirement that no four consecutive segments overlap. Of course the propagator scheme is used for the summation of all conformations, but the result of that will not differ from the evaluation of Eq. (1) for each conformation separately. It is subsequently trivial to find the segment density distribution for a given segment type A,

$$\varphi_A(z)=\sum_i \sum_s \varphi_i(z,s)\delta^A_{s,i}, \tag{2}$$

where $\delta^A_{s,i}$ is the chain architecture operator which assumes the value unity when segment s of molecule i is of type A and zero otherwise. In Eq. (2) the summation over the molecule types i is included to have a general equation. The segment-type distribution functions are used below, i.e., in the equations for the segment potentials.

From segment potentials to segment densities for water

In principle, Eq. (1) can be applied to monomeric compounds. Indeed in the system discussed below there are small ions such as Na^+ and Cl^- which are composed of just one segment. For such monomer of type X the densities are proportional to the Boltzmann weight,

$$\varphi_X(z)=\varphi^b_X e^{-u_X(z)/k_BT}=\varphi^b_X G_X(z), \tag{3}$$

where in this case the normalization is given by the bulk volume fraction of component X, φ^b_X which either is an input quantity or, when the amount of the component is given, is the outcome of the calculations.

For the water molecules the same procedure could in principle be followed. However, it was found that using featureless monomer solvent molecules resulted in too high water concentrations in the bilayer. The physical reason for these high water concentrations in the bilayer was also evident. If water is modeled as a small unit that interacts isotropically, in a Bragg-Williams manner, with its surroundings, the mixing entropy term will prevent very low local concentrations. One way to solve this problem is to account for orientation-dependent interaction in water on a quasichemical approach, such as pioneered by Besseling [29]. In such a method it becomes rather complicated, however, to deal with chain molecules and therefore it is necessary to resort to more pragmatic models.

The important property of water molecules is that it can form H bonds with neighboring water molecules. Effectively such H bonded water molecules behave as larger clusters. This stimulated us to formulate a simple model for water, which is readily incorporated in the formalism outlined above. The key idea is to allow for the water molecules to cluster and these clusters operate as separate kinetic units. Let us assume that the clustering depends only on the local water density and is not influenced by the gradient in density in the z direction. Then the clustering will depend only on the local z coordinate. As the clustering will be restricted to occur in a layer the z coordinate is omitted in the following equations. Let the density of water that follows from Eq. (3) be indicated by φ^1_1, where the superindex 1 is referring to the size of the cluster, being unity in this case. Introducing a cluster constant K and the probability to have a cluster with size m be given by Φ^m, the following equilibria:

$$\Phi^m+\Phi^1 \leftrightarrow \Phi^{m+1}, \quad \forall \quad m>0 \tag{4}$$

are assumed to exist, where $K=\Phi^{m+1}/(\Phi^m\Phi^1)$, for all $m>0$. Equation (4) generates an equilibrium between monomers ($m=1$), dimers ($m=2$), trimers ($m=3$), etc. It is easily shown that the water density of monomers φ^1_1 is related to the overall water density φ_1,

$$\varphi_1=\sum_m \varphi^m_1=\sum_m m\Phi^m=\frac{\Phi^1}{(1-K\Phi^1)^2}=\frac{\varphi^1_1}{(1-K\varphi^1_1)^2}, \tag{5}$$

where $\varphi^m_1=m\Phi^m$ is the volume fraction due to water molecules that belong to clusters with size m. Equation (3) can still be used to obtain the monomer water density: $\varphi^1_1=\varphi^{1,b}_1 G_1$, where $\varphi^{1,b}_1$ is the monomer water density in the bulk. If the total water volume fraction in the bulk φ^b_1 is known, one can use Eq. (5) to find the corresponding monomer volume fraction of water in the bulk,

$$\varphi^{1,b}_1=\frac{1}{K}+\frac{1-\sqrt{4K\varphi^b_1+1}}{2K^2\varphi^b_1}. \tag{6}$$

Inspection of Eq. (5) shows that if the cluster constant K is large, the presence of free monomers of water is strongly suppressed. Effectively, only the free monomers can partition into the bilayer and the model therefore has the desired effect that the water molecules will avoid the membrane interior.

From segment densities to segment potentials and bond-orientation weighting factors

Recall that the procedure outlined above to find the volume fraction distributions assumed that the segment potentials and the bond-orientation weighting factors were known. The key element of a self-consistent-field theory is that these quantities in turn follow from the segment distributions. In this section we will subsequently assume that all density distributions and the distribution of bonds in the system are known. When this is the case, the potentials as well as the bond weighting factors follow straightforwardly. Again we follow Meijer *et al.* [28] and only pay some more attention to the point where we deviate from this work.

It follows from differentiation of the mean-field partition function that the segment potentials are composed of four terms,

$$u_A(z)=u'(z)+u^{FH}_A(z)+u^{elec}_A(z)+u^{pol}_A(z), \tag{7}$$

where it is understood that $u_i(z,s)=\Sigma_A u_A(z)\delta^A_{i,s}$. In Eq. (7) $u'(z)$ is a Lagrange field coupled to the constraint that in each lattice layer, each lattice site is, on average, filled exactly once: $\Sigma_A\varphi_A(z)=1$. This means that on a site there can be a segment of the lipid molecule, one of the ions, a water unit or a unit V which represents a free volume site.

The second term in Eq. (7) accounts for the short-range nearest-neighbor contact energies which are computed by making a Bragg-Williams approximation. This means that

the probability to find a contact between segments A and B is given by the product of the volume fractions. From this it follows that

$$\frac{u_A^{FH}(z)}{k_BT}=\sum_B \chi_{AB}([\varphi_B(z-1)+\varphi_B(z)+\varphi_B(z+1)]/3-\varphi_B^b)$$

$$=\sum_B \chi_{AB}(\langle\varphi_B(z)\rangle-\varphi_B^b). \quad (8)$$

Here the contact interactions are parametrized by the well-known Flory-Huggins interaction parameters $\chi_{AB}=(2/k_BT)(2U_{AB}-U_{AA}-U_{BB})$, where $U_{xx'}$ is the interaction energy between units x and x'. From this definition it is seen that the reference for the interactions is that between like segments. Perhaps it would intuitively be more easy to take as the reference all the interactions with the V compound. The translation to this scheme is not difficult. As it does not affect the results in any way, we prefer to keep the χ parameters as presented in Eq. (8). Equation (8) defines the angular brackets notation as a three-layer average density. The reason for this average is that it is possible for a segment not only to make contacts with segments in the same layer, but also with segments in the neighboring layers. Further, the homogeneous bulk density (dilute in lipids and rich in water) is used as a reference for the segment potential.

The third term in Eq. (7) is the familiar electrostatic term,

$$u_A^{elec}=\nu_A e\psi(z), \quad (9)$$

where ν_A is the valence of the segment of type A, e is the elementary charge, and ψ is the electrostatic potential. The electrostatic potential follows from the Poisson equation for which it is necessary to know the charge distribution

$$q(z)=\sum_A \nu_A\varphi_A(z)e \quad (10)$$

and the dielectric permittivity profile. For the latter, a volume fraction weighted average of the segment contributions ε_{rA} is used,

$$\varepsilon(z)=\varepsilon_o\sum_A \varepsilon_{rA}\varphi_A(z). \quad (11)$$

This equation guarantees that the local relative dielectric constant in the aqueous phase will be near 80 and in the center of the bilayer near 2. Of course, a discretized version of the Poisson equation must be used,

$$\frac{\partial\varepsilon(z)\partial\psi(z)}{\partial z^2}=-q(z). \quad (12)$$

At both boundaries the electric field $E(z)=-\partial\psi(z)/\partial z$ is zero, which then guarantees that the system will remain overall electroneutral. Of course, the electrostatic potential is zero in the reference bulk.

The last term in Eq. (7) is new. We are not going to derive this new term here. Instead a qualitative argument why the new term should be included will be given. Physically the segment potential must express the work per segment that needs to be performed for taking a segment from the bulk, where there is no electric field, to the interfacial zone where there is a given electric field. When a segment is transported it will be polarized by the electric field. The magnitude by which this takes place is proportional to the electric field and the dielectric permittivity of the segment. The gain in energy due to this polarization is also proportional to the electric field and therefore there is a polarization contribution proportional to $-\varepsilon_{rA}E^2$. The polarization of the molecule has also an entropic consequence. It can be shown that the free energy effect for the polarization, which should be included in the segment potential, is just half this value, $-\frac{1}{2}\varepsilon_{rA}E^2$. On the lattice the electrostatic potential and not the field strength is known in each layer and one can use Eq. (12) to derive the appropriate lattice equation for the polarization term,

$$u_A^{pol}(z)=\varepsilon_{rA}\left[\frac{\varepsilon(z)}{\varepsilon(z-1)+\varepsilon(z)}[\psi(z-1)-\psi(z)]^2+\frac{\varepsilon(z)}{\varepsilon(z+1)+\varepsilon(z)}[\psi(z+1)-\psi(z)]^2\right]. \quad (13)$$

It can be shown that when the dielectric constant profile does not depend on the molecular distribution, term 4 in Eq. (7) can be incorporated in the Lagrange field. This explains why in the standard Poisson-Boltzmann theory the polarization term is never included. In our model it is possible to prove that this term is needed because in absence of this term, the test for internal thermodynamic consistency, i.e., the Gibbs equation test, fails.

The final problem that needs to be discussed is the bond-orientation weighting factors. Here we follow again the approach of Meijer *et al.* [28] exactly. Recall that the total number of bonds of molecule i is given by N_i-1, and the volume fraction of molecule i in the bulk by φ_i^b. The probability to find a segment in the bulk which has a bond connected to it, $\varphi^{b\sigma}$, is then given by

$$\varphi^{b\sigma}=\sum_i \frac{N_i-1}{N_i}\varphi_i^b. \quad (14)$$

Let the coordination number of the lattice be given by Z (for a tetrahedral lattice $Z=4$). This means that the number of possible bonds is Z. One half of these bonds are within the layer, the other half is between the layers. Now the anisotropic bond-weighting factors for bonds that are present between layers z and z', $G(z|z')=G(z'|z)$, depend primarily on the fraction of segments in layer z which have a bond towards layer z'. This quantity follows directly from proper summation of the densities in the stage in which bond information is (still) available, i.e., from $\varphi(z,s^{\alpha\beta})$, where both α and β refer to the directions of the bonds on segment s. Let us denote by $\varphi(z|z')$ the fraction of the volume taken up by bonds between layers z and z'. Now the anisotropic bond-weighting factors are given by

$$G(z|z+1)=G(z,h)=\frac{1-\frac{2}{Z}\varphi^{b\sigma}}{1-\varphi(z|z+1)},$$

$$G(z|z)=G(z,f)=G(z,g)=\frac{1-\frac{1}{Z}\varphi^{b\sigma}}{1-\varphi(z|z)/2}, \qquad (15)$$

$$G(z|z-1)=G(z,e)=\frac{1-\frac{2}{Z}\varphi^{b\sigma}}{1-\varphi(z|z-1)}.$$

In these equations the numenator is a normalization quantity which ensures that in the isotropic bulk $G(z|z')=1$, whereas the denominator is the ''active'' part of the equation. Inspection shows that the anisotropic weighting factor diverges when $\varphi(z|z')\to 1$ (for $z'\neq z$). This limit cannot exactly be reached because there are always chain ends or monomeric compounds at each layer z, but it indicates that, when the system is locally aligned, there will be a local bond-weighting factor that is very large. This, in its turn, will ensure that the ''test'' chain will follow with higher probabilities the local direction of the other molecules in the system. (This is what happens when the membrane system is in the gel phase.) The division by 2 in the denominator for the bond-weighting factor for bonds that remain in the layer originates from the assumption that the bond directions remain isotropic within the layer. Therefore, only half the bonds effectively lay parallel to the bond that is put in the layer. This mean-field assumption has the consequence that it is not possible to find crystallization along the membrane surface in the present model.

The SCF solution and the thermodynamics of free flying membranes

In the previous sections it was shown that the SCF formalism gives a strategy how to compute the segment density and bond density profiles from the segment potentials (including the polarization contribution and the electrostatic potential). On the other hand the segment potentials as well as the electrostatic potential and the polarization contribution can be computed from the segment density and bond direction profiles. A fixed point of these two parts of the calculations is characterized by the fact that the potentials that are used to compute the densities are recovered when they are evaluated from the densities. Besides this self-consistent-field requirement it is necessary to force that all lattice sites, also in the reference bulk system, are filled. Only for a particular choice for the Lagrange field profile, this constraint is fulfilled. Then a solution of the equations is accepted. Typically, the precision found for the segment densities is seven significant digits, for which (depending on the initial guess) only on the order of 100 sec CPU time is needed on a personal computer.

For any SCF solution it is then possible to compute the thermodynamic characteristics of the system. Of interest in the present study is the evaluation of the surface tension of the bilayer. For this it is necessary to compute the lateral pressure profile $\pi(z)$. It is well known that, in general, the lateral pressure has nonlocal contributions and that it is arbitrary how to assign the nonlocal contributions of the lateral pressure to a particular coordinate. This is the case in the present model as well. However, the surface tension, which is found after appropriate summation over the lateral pressure,

$$\gamma\not{\ell}^2=-\sum_z \pi(z), \qquad (16)$$

does not depend on the choices made for the assignments. When the nonlocal terms in the lateral pressure are evenly distributed over the coordinates involved, the following expression for the lateral pressure is obtained:

$$-\frac{\pi(z)}{k_BT}=2\ln G(z|z)+\frac{\ln G(z|z-1)+\ln G(z|z+1)}{2}+\left[\varphi_1(z)-\varphi_1^b-\frac{\varphi_1^1(z)}{1-K\varphi_1^1(z)}+\frac{\varphi_1^{1,b}}{1-K\varphi_1^{1,b}}\right]+\sum_A \varphi_A(z)u_A(z)+\tfrac{1}{2}\sum_A\sum_B \chi_{AB}\{\varphi_A(z)(\langle\varphi_B(z)\rangle-\varphi_B^b)-\varphi_A^b(\varphi_B(z)-\varphi_B^b)\}+\frac{1}{2k_BT}q(z)\psi(z). \qquad (17)$$

With respect to the equation given by Meijer *et al.* [28], only the term in the square brackets is new. This line is the appropriate contribution coming from the distribution of the water molecules. The indicated terms originate from the quantity $\Sigma_m[\varphi_1^m(z)-\varphi_1^{m,b}](1-1/m)$ which is the usual chain entropy contribution to the lateral pressure, i.e., not having the orientational-dependent weighting factors. The factor 2 in the first term on the right-hand side of Eq. (17) originates from the fact that there are bonds in both the f and g directions. The division by 2 in the second term originates from the fact that the lateral pressure contribution is equally divided between neighboring layers. The other terms in Eq. (17) are standard, where it is understood that the potential field $u_A(z)$ now includes the polarization term mentioned above. Note that in the last two terms there are explicit choices made as to the assignment of contributions to the lateral pressure. Again, these choices are of no consequence for the surface tension, but are of course affecting the local value of the lateral pressure significantly [25].

Again, for every SCF solution it is possible to evaluate the surface tension of the bilayer. From a thermodynamic analysis for free standing bilayers it follows that the surface tension should be zero. In principle, however, one needs to search for such an equilibrium point, because this equilibrium point only occurs for a particular well-defined area per lipid molecule in the bilayer. To obtain such equilibrium point it is necessary to compute the surface tension as a function of the amount of lipids in the system and select from this the tension-free case. Below we will report on the

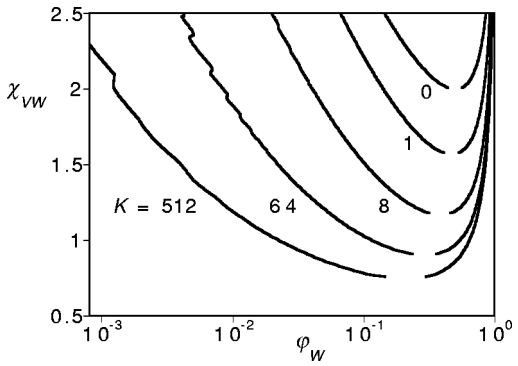

FIG. 1. Water-vapor phase diagram for various values of the cluster constant K as indicated. In these phase diagrams χ_{VW} plays the role of the inverse temperature. The densities are presented on a log scale. The irregularities of the binodal lines at high values of the χ_{VW} parameter are due to lattice artifacts.

structure of the bilayers for which the surface tension is negligible, i.e., $|\gamma\ell^2|/k_BT<10^{-5}$.

RESULTS

The water model

Let us first discuss the water-vapor phase behavior. This phase behavior is essential, because the self-assembly of the lipids is invariably linked to the water-vapor properties. From the known phase diagram it is then possible to select acceptable parameters for the water phase. These parameters will be used in the remainder of this paper.

Let us thus consider the system of water, W, in a free-volume component which is referred to by the letter V. The free-volume compound is modeled as a featureless unit with a volume equal to one lattice site. In this system there are two parameters. The first one is the cluster constant K. Physically one can argue that K is related to ΔG of a H bond, which is several k_BT units. The second parameter is the Flory-Huggins interaction parameter χ_{VW}. When this value is sufficiently large, it will be the case that there is a solubility gap. This means that, at appropriate compositions, there will be both a V phase and a W phase. It is possible to numerically evaluate the corresponding binodal conditions.

In Fig. 1 the phase diagram in terms of the interaction parameter χ_{VW} and the binodal densities for various values of the cluster constant are presented. When $K=0$, the water phase is modeled as a simple monomer and the Flory-Huggins theory applies. The critical point is exactly at $\chi_{VW}=2$ and the critical density is $\varphi_W=0.5$; the phase diagram is completely symmetric. With increasing value of the cluster constant the water clusters in the system increase in size, particularly in the water phase. The phase diagram becomes progressively more asymmetric implying that much less water is found in the V phase, than free volume in the water phase. The critical point shifts to lower values of the interaction parameter χ_{VW} and approaches $\chi_{VW}=0.5$ for very large K values. The critical density also drops to lower values. This is natural, as the water effectively behaves as a polydisperse ''polymer'' system. Relatively small values for the K value already have a dramatic effect.

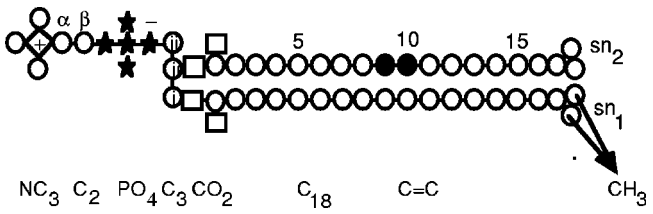

FIG. 2. The graphical representation 1-stearoyl-2-oleoyl-*sn*-glycero-3-phosphatidylcholine used. The open spheres are either CH_2 or CH_3 groups, the closed spheres represent the C=C unsaturation (double bond of *cis* configuration on position 9) along the acyl chain. The open squares represent oxygen, the stars represent the phosphate group and finally the diamond represents the nitrogen atom. The numbering of the carbons along the *sn*-1 and *sn*-2 tail, the carbons in the glycerol backbone and the carbons between the nitrogen and phosphate group are indicated. The two spheres at the end of the chains represent the single unit CH_3. The positive charge is located at the nitrogen and the negative charge is distributed over the five units of the phosphate group. In the molecule of 1-stearoyl-2-docosahexaenoyl-*sn*-glycero-3-phosphatidylcholine, the *sn*-2 chain contains 22 carbons and the double bonds of *sn*-2 chain are located on 4, 7, 10, 13, 16, and 19 positions.

Because high values of the K value give problems with numerical convergence (cf. the irregularities in Fig. 1 for high K and high χ_{VW} values), it was decided to select a reasonable value: $K=50$. It is known that at room temperature the water-vapor system is far from the critical point and therefore a sufficiently high value for the interaction between V and W was chosen: $\chi_{VW}=2.5$. For this set of parameters it was found that, at coexistence, the volume fraction of V in the water phase equals $\varphi_V^{(W)}\approx 0.042\,475$. The amount of water in the V phase is about a factor of 10 less: $\varphi_W^{(V)}\approx 0.005\,06$. Of course it would have been better to take a higher K value such that the experimental values for the free volume in the water phase and amount of water in the vapor phase could have been approached. At this stage, however, we need to settle with the qualitative effect, which is reasonable because true water is of course much more complicated than assumed in our model.

Parameters for the SOPC and the SDPC systems

Having fixed the K value for water, the appropriate value for χ_{VW}, and the corresponding value of the density of V in the water phase, the stage is set to introduce the corresponding parameters for the lipid molecules. For densely packed layers it is essential that the excluded volume (i.e., the intrinsic volume) is realistically represented. In Fig. 2 a graphical representation is made of 18:0/18:1 PC molecule. Each unit drawn in this presentation is a segment which occupies exactly one lattice site. The carbons (open spheres) in the head group between the choline and the phosphate are numbered α, β. The carbons of the glycerol backbone are numbered i, ii, and iii, where the *sn*-1 chain is grafted on the carbon i and the *sn*-2 chain on carbon ii. Halfway along the *sn*-2 acyl chain there is a *cis* double bond indicated by the black spheres. (The *sn*-2 chain in SDPC differs with respect to the unsaturated bonds as discussed in the legend of Fig. 2.) The

end of the acyl chain is a branched unit which is interpreted as the CH_3 group. This is the way how the important fact that the CH_3 group significantly differs from a CH_2 group [30] is implemented. In the present model this is only applied to the ends of the acyl chain, not to CH_3 groups in the choline head group. In principle, the CH_3 groups may interact differently with its surroundings than CH_2 groups. For this disparity a few choices will be discussed shortly.

An important quantity is the interaction parameter between the hydrocarbon units and water $\chi_{\text{C-H}_2\text{O}}$. The value for this parameter is estimated by the usual method that the CMC, as predicted by the SCF model, follows experimental facts for a series of surfactants with increasing tail length. This occurs to a good approximation (not shown) for $\chi_{\text{C-H}_2\text{O}}=0.8$. It is noted that this value is much lower than in previous calculations where water was assumed to be a structureless unit. The second important parameter is the interaction of the carbon with the *V* units. From lipid monolayers on the air-water interface it is known that the hydrocarbon units prefer the *V* phase over the water phase. This does not directly suggest that the solvent quality is good; this would imply that the lipids would easily evaporate. Thus, it is natural to also select a reasonably strong repulsion between C and V. It is important to mention that the purpose of this paper is to discuss bilayers in the liquid-crystalline state. In this context it is of key importance to select an appropriate value for $\chi_{\text{C-V}}$. Very high values for this quantity will introduce little free volume in the bilayer and the bilayer will be in the gel state. Too low values on the other hand will effectively suppress the gel state completely. A value of $\chi_{\text{C-V}}=2$ is chosen which introduces just enough free volume in the bilayer to suppress the gel state. It is not excluded that, when it is necessary to revisit the gel-to-liquid phase transition phenomenon, it will prove to be necessary to tune the $\chi_{\text{C-V}}$ to a more accurate value. One of us has argued in another work that the CH_3 group prefers the *V* phase over the CH_2 groups [31]. Indeed, this is consistent with MD force fields [32] and this is implemented in the present work by setting $\chi_{\text{CH}_3\text{-V}}=1$ and a small repulsion between the CH_3 and CH_2 groups. The interaction between CH_3 and O is also made somewhat more repulsive than for CH_2 and O. The complete set of parameters is collected in Table I.

It is essential to mention that the choline group is positively charged. Following Meijer *et al.* [28], a full positive charge is placed on the nitrogen. On the other hand, the phosphorus group is composed of five equivalent units which are all named P. The charge is distributed evenly over these units. Finally, there are oxygen atoms in the carbonyl group. In Fig. 2 these groups are indicated with an open square. These units are given hydrophilic properties and because they lack a charge, it was chosen to give them somewhat intermediate properties.

Although the PC head group is zwitterionic, it is not necessary to add salt. However, some salt was added in the SCF case. The bulk concentration of Na^+ and Cl^- was fixed to $\varphi^b_{\text{Na}}=\varphi^b_{\text{Cl}}=0.01$. Of course this is a high value, but it was shown for calculations on DMPC that the membrane is not extremely sensitive to the ionic strength [22]. A high ionic strength reduces the electrostatic screening length and simplifies the calculations. The charged components repel the hydrocarbon phase as well as the *V* components and therefore receive a high χ parameter. All remaining χ parameters are less important and for this reason they were put to zero. This means that enthalpic interactions between water and ions, water and charged units in the head group, and between the N and P head-group units are ignored. Of course this is an idealization of the system and nonzero values for these parameters should be considered when the effects of particular ions on the membrane properties are of interest.

TABLE I. Parameters used in the SCF calculations. In the first row the relative dielectric constant for the compound is given. In the second row the valence of the unit is given. Remaining parameters: (*b*) The characteristic size of a lattice site 0.3 nm. The *K* constant for water association: $K=50$. The energy difference for a local *gauche* conformation with respect to a local *trans* energy: $\Delta U^{tg}=0.8k_BT$. The volume fraction in the bulk (pressure control) of free volume was fixed to $\varphi^b_V=0.042\,575$.

−	H_2O	V	C	CH_3	N	P	O	Na	Cl
ε_r	80	1	2	2	10	10	10	10	10
ν	0	0	0	0	1	−0.2	0	1	−1
χ	H_2O	V	C	CH_3	N	P	O	Na	Cl
H_2O	0	2.5	0.8	0.8	0	0.5	0	0	0
V	2.5	0	2	1	2.5	2.5	2.5	2.5	2.5
C	0.8	2	0	0.5	2.6	2.6	2	2.6	2.6
CH_3	0.8	1	0.5	0	2.6	2.6	2	2.6	2.6
N	0	2.5	2.6	2.6	0	0	0	0	0
P	0.5	2.5	2.6	2.6	0	0	0	0	0
O	0	2.5	2	2	0	0	0	0	0
Na	0	2.5	2.6	2.6	0	0	0	0	0
Cl	0	2.5	2.6	2.6	0	0	0	0	0

Important for the electrostatics is the dielectric permittivity. For water a relative dielectric constant of 80 was used, the hydrocarbon units have a value of 2, the *V* component has a value of 1, and for all other units a value of 10 is used (see also Table I). Finally, it is necessary to specify the value for the difference in energy between *gauche* and *trans* configurations along the chain. Throughout the chain a value of $\Delta U(t)=0.8k_BT$ is used except for the double bonds for which the *gauche* state has the lowest energy: $\Delta U(\text{C=C})=-10k_BT$. The classical notion of *gauche* and *trans* conformers is lost for bonds that are connected to a branch point. There is no point in assigning differences in energy for local bond orientations and therefore a value of $\Delta U=0k_BT$ is used for all these bonds, irrespective of how these are oriented. Of course the local excluded-volume effects are obeyed, which means that the bonds on the branch point do not overlap.

In all cases the membranes are a distance $d=80\ell$ apart. For high ionic strengths such as in the present system, this is large enough to have isolated noninteracting bilayers. For the electrostatic calculations [cf. Eqs. (12) and (13)], it is necessary to choose a value for ℓ. This molecular length was set to $\ell=0.3$ nm, which is about the value for the size of a water molecule and it is an appropriate value for the water

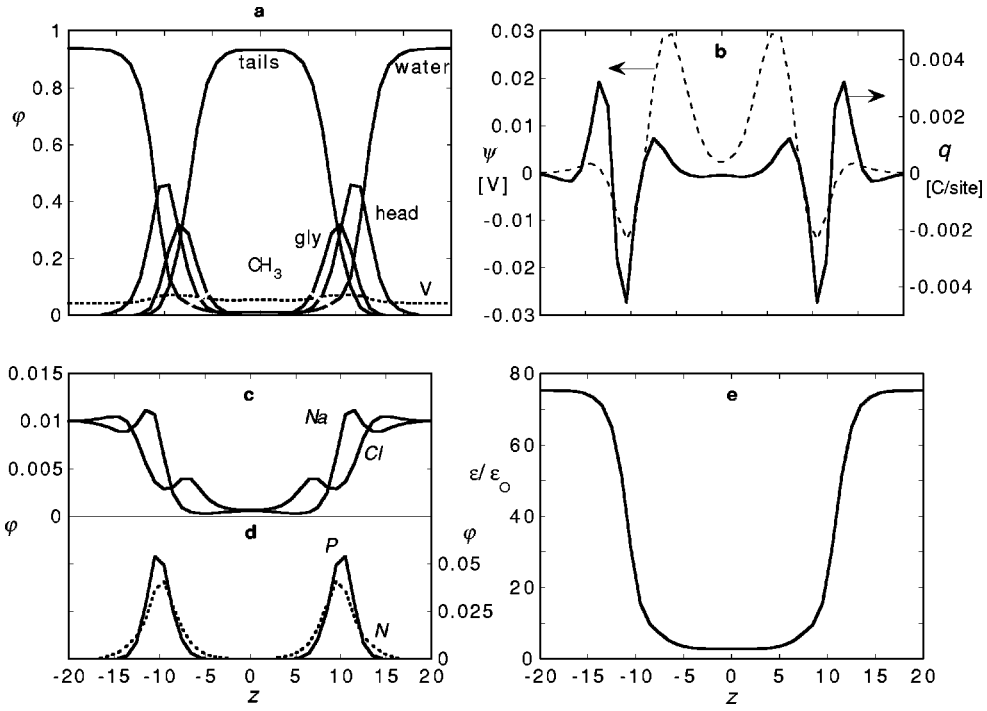

FIG. 3. (a) The overall density profiles across the SOPC bilayer for the water, free volume, and the main lipid fragments: the head group, the tails, the glycerol backbone, and the CH_3 units as indicated. The center of the bilayer has the coordinate $z=0$. (b) The electrostatic potential profile across the bilayer (left ordinate), and the overall charge profile (right ordinate). (c) The density profile for the monovalent ions Na and Cl (left ordinate). (d) The volume fraction profiles of the nitrogen of the choline group and the central P of the phosphate group (right ordinate). (e) The dielectric permittivity profile across the bilayer.

phase. For the membrane units, and therefore for the membrane phase this value should more likely be chosen slightly lower. Below, the value of ℓ is kept in the results and it is suggested that this value is still adjustable in the range $0.2<\ell<0.3$ nm, which gives the opportunity to scale the SCF results to a particular MD (or experimental) result for a well-documented case.

Parameters mentioned in this section will be used in the first part of the Results section. In the second part we will show some effects of variations in this parameter set.

SCF results for SOPC and SDPC bilayers

The SCF predictions will be presented in this section and the corresponding MD predictions are collected in the subsequent one. Let us first analyze the overall features of the SOPC bilayer.

In Fig. 3 the volume fraction distributions of the major components in the system are given as well as the electrostatic potential profile and the charge density profile (of free charges) across the bilayer. The z coordinates are in units of the size of the lattice site, ℓ, and the numbering is chosen such that the center of the bilayer coincides with the value $z=0$. From Fig. 3 several important results can be extracted. One of them is the thickness of the bilayer. The value for this quantity depends strongly on the exact definition. When the thickness H of the bilayer is defined as the distance between the points where the head-group densities on either side of the bilayer drop to (nearly) zero, a value of approximately $H\approx 30\ell$ is found. Alternatively, where the maximum of the head-group densities on each bilayer leaflet is used, a value of approximately $H\approx 20\ell$ is found. The average (first moment) distance between the P groups is found to be $d_{PP}=19.93\ell$. The area per lipid molecule in the bilayer on the other hand, can unambiguously be computed and this value is $a_o=10.044\ell^2$.

From Fig. 3(a) it is noticed that the amount of water in the hydrophobic region of the bilayers is very small and drops to a value of about 0.01. It is expected that this value is still an overestimation, but this result is much more reasonable than the predictions from the model of Meijer et al. [28]. The water phase penetrates not very far into the bilayer. In line with common knowledge the border between the hydrophilic and hydrophobic region is the glycerol backbone region. These groups are, as expected, situated between the tails and the head groups. A significant overlap of the glycerol backbone profile with that of the tails and the heads is predicted. The tail profile in Fig. 3(a) includes all the carbon atoms in the two acyl chains. Inspection of this profile reveals a minor dip in density at the central region of the bilayer. The CH_3 end groups show a rather broad distribution. The maximum of this distribution is at the center of the bilayer. Of course there are chains that cross the interface as will be discussed below. The free volume profile is nontrivial. There is a local maximum in the center of the bilayer and more pronounced there is a maximum at the interface between the head groups and the glycerol backbone. This maximum coincides with the position of the hydrophobic-hydrophilic phase boundary.

In Fig. 3(b) the electrostatic potential profile is shown in combination with the corresponding charge density profile.

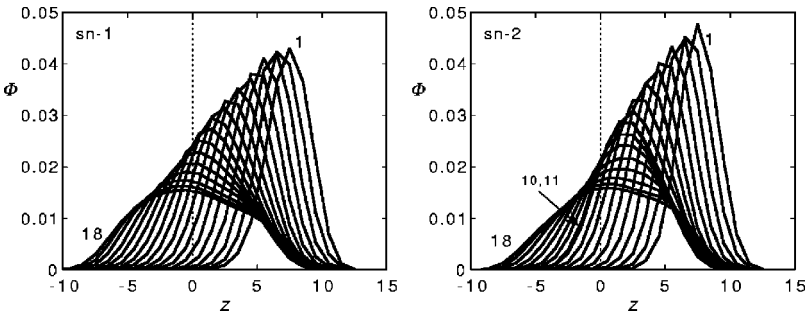

FIG. 4. Segment density profiles for individual segments of the sn-1 (left panel) and sn-2 (right panel) chains of SOPC bilayers. Only those distributions are shown for the chains which have the nitrogen of the head group on a positive coordinate. For ease of comparison the density profile of the CH_3 group is divided by 2. The center of the bilayer is indicated by the vertical line.

This last profile is composed of the four contributions given in Figs. 3(c, d). It is of no surprise that the number of charges inside the bilayer is very small indeed. Both the ions as well as the phosphate and choline group avoid the apolar phase where the dielectric constant is very low.

Let us first evaluate the position of the head groups which can be deduced from Fig. 3(d). It is seen that the distribution of the nitrogen and the central phosphate have their maximum on almost the same z position. This means that, on average, the head group is oriented almost parallel to the membrane surface. This result is in line with experiments: an approximate average tilt angle of the phosphorus-nitrogen dipole in a fluid 18:1/18:1 PC bilayer (determined by joint refinement of x-ray and neutron diffraction methods) was $22° \pm 4°$ with respect to the bilayer surface [33]. It is in reasonable agreement with the value of 18° obtained from 2H nuclear magnetic resonance and Raman spectroscopic studies of 16:0/16:0 PC [34]. There are other experimental data that the polar head groups are approximately parallel to the surface [35–37]. According to the calculations of model PC bilayer [38] the polar head group has $a \approx 15°$ angle of inclination to the bilayer surface. The SCF result discussed is also in line with previous results from DMPC membranes [20].

Furthermore, the choline group has a more wide distribution. This is natural because end groups in a chain have more possibilities to sample the space and are the locus of relatively high conformational entropy. It has been shown before that the width of the choline distribution decreases with decreasing ionic strength [20]. As a consequence, the electrostatic potential is not only positive on the outside, but also positive inside and has a negative region at the position of the phosphate group. The small ions in the system follow the electrostatic potential by way of the appropriate Boltzmann factor. At the center the electrostatic potential drops to almost zero and consequently the concentration of Na and Cl becomes almost identical.

In the same context it is of interest to present the dielectric permittivity profile across the bilayer membrane as well. In Fig. 3(e) this profile is given. Of course this profile closely follows the water distribution. In the water phase the dielectric constant is close to 75. The deviation from 80 is due to the free volume in the water phase which is close to 4.25%. As anticipated, the relative dielectric constant in the center of the bilayer is low. Numerical evaluation gives a value near 2.8.

For a more detailed analysis of conformations of the acyl chains one should realize that the overall distributions are the result of contributions of both monolayers of the bilayer. It is not too difficult to evaluate the distribution function for those molecules that have their head group on the positive side of the coordinate system. Let us thus denote the density profile of the molecules of the right leaflet as $\Phi(z,s) = \varphi(z,s|z' > 0,s')$ where the position of s' determines to which side of the leaflet the molecule belongs to. The nitrogen group has been selected for s'. In Fig. 4 such profiles of all segments of both tails are shown. The center of the bilayer is exactly at $z=0$. Of course the two tails have not identical conformations in the bilayer. It is known that this is already the case for fully saturated lipids, because the head group is asymmetrically coupled to the glycerol backbone. In such bilayer the sn-2 tail penetrates just a bit less deep into the bilayer than the sn-1 chain. From Fig. 4 it is easily seen that this is also true for SOPC bilayers. In line with previously obtained results the distribution is most narrow for the segments near the glycerol backbone and becomes wider at the chain ends. Each distribution may be characterized by a maximum value Φ^{max} which occurs at a particular coordinate z^{max}. For the sn-1 chain it is interesting to note that $\Phi^{max}(z^{max})$ is a smooth curve, which near the outside of the bilayer approaches a straight line and drops to a low Φ^{max} value near $z^{max}=0$.

In the SOPC lipid the sn-2 tail is unsaturated. As mentioned above the *cis* double bond is introduced in the chain by forcing a *gauche* conformation at the C8—C9═C10—C11 position. This means that, e.g., if the C9═C10 bond lies parallel to the z direction, either the C8—C9 or the C10—C11 bond is forced to lie perpendicular to the membrane director. However, the chain still has many options to position the *gauche* conformer and therefore the outcome is not trivial. Inspection of Fig. 4 shows that C10 and C11 have very similar distributions. This suggests that the C8—C9 and the C9—C10 bonds are preferentially aligned in the z direction. Apparently, the segments with the high ranking number (towards the tail end) are conformationally perturbed with respect to the saturated case. In other words the free end must ''correct'' for the alignment problem introduced by the double bond. The signature of the double bond may also be seen in the $\Phi^{max}(z^{max})$ curve. Especially near $s=10$ a drop in Φ^{max} is found. As a result a significantly less smooth curve is found.

It is of interest to notice that the maximum of the distribution for the chain end of the sn-1 chain is just at negative z coordinates. This means that the chains cross the center significantly. However, the distribution is asymmetric and it

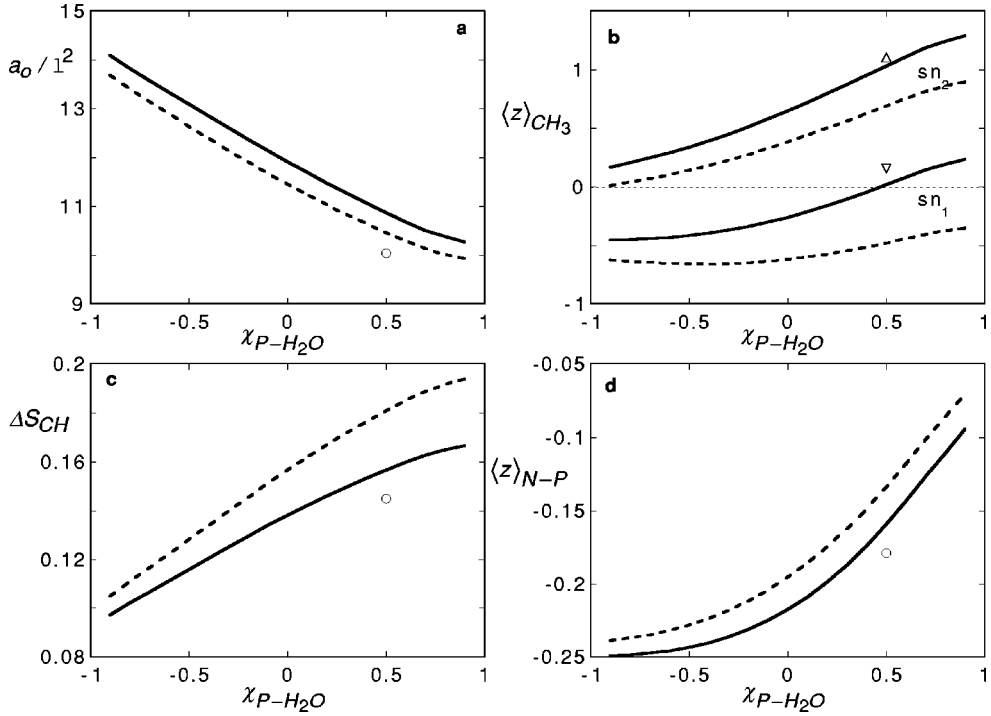

FIG. 5. Parameter study for SOPC bilayers. (a) The area per molecule in units of ℓ^2, (b) the average position of the CH_3 end group of the sn-1 and sn-2 chain as indicated, (c) the value of the order parameter of the $s=10$ segment of the saturated tail minus that of the corresponding segment of the unsaturated chain, (d) the difference in average position of the N of the choline group and the phosphate group as a function of $\chi_{\text{P-H}_2\text{O}}$. The solid lines are for the case that the CH_3 group has twice the volume of a CH_2 group. The dashed lines are for equal volumes of the CH_3 and CH_2 groups. $\chi_{\text{CH}_3\text{-CH}_2}=0$, $\chi_{\text{CH}_3\text{-O}}=2$ and $\chi_{\text{CH}_3\text{-V}}=2$ and other parameters as in Table I. The symbols in the figure refer to the (reference) results for the membrane analyzed in the Figs. 3 and 4.

turns out that the average position remains positive as will be discussed below. This is a significant result. It shows that one can classify these bilayers as being noninterdigitated. This is an important property of the present model. In previous work always strongly interdigitated bilayers were found [21].

The effects of changes in the parameter set of the SCF approach

It is important to know how sensitive the SCF results are for changes in the parameter set. To monitor this sensitivity, four properties of the membrane are selected. The first one is the area per molecule which is inversely related to the membrane thickness. The second one is the average position of the CH_3 end group of the acyl chains. This quantity gives insight in the amount of interdigitation of the acyl chain. The third one is the orientation of the head group characterized by the difference between average position of the N and the P. The final property that is analyzed has to do with the segmental order parameters. In short, when the segment order parameter is high, the chain is locally aligned perpendicular to the membrane surface. If it is low (near zero), the chain fragment is most likely randomly oriented. For a more accurate definition and for more details of the order parameters we refer to Ref. [2]. The double bond in the acyl chain has an effect on the local ordering. To quantify this we choose the order parameter at the position of the double bond and compare this with the order parameter of the corresponding segment on the saturated chain. The fourth aspect that will be discussed below is therefore the relative drop of the segmental order parameter of the unsaturated chain.

Without mentioning otherwise it is assumed in this section that CH_3 and CH_2 have identical χ-parameters and thus that $\chi_{\text{CH}_3\text{-CH}_2}=0$, $\chi_{\text{CH}_3\text{-O}}=2$ and $\chi_{\text{CH}_3\text{-V}}=2$. This operation eliminates one row and one column in the parameter matrix as given in Table I. The solid lines in Fig. 5 are for the case that the CH_3 group has double the volume of a CH_2 group. The dashed line corresponds to the case that both groups have equal volume and the model reduces (regarding the chain ends) to the one used in previous studies.

In Fig. 5 the mentioned membrane characteristics are plotted as a function of the $\chi_{\text{P-H}_2\text{O}}$. This parameter is used because of its effects on the ''effective'' hydrophilicity of the head group. Many of the trends presented in this graph are easily explained. The area per head group in the bilayer is a decreasing function with increasing hydrophobicity taken for the phosphorus group as shown in Fig. 5(a). This is the case because the head group will not solvate as much as in the hydrophilic case. The predicted effect is rather large. The drop in area shown in Fig. 5(a) is from 14 to 10 units ℓ^2. When the membranes become thinner with increasing hydrophilicity of the head group, the tails can more easily cross the membrane center. Indeed Fig. 5(b) shows that the average position of the end of the sn-1 chain can become negative. This means that the chain is crossing the center with the end segment and correspondingly several other segments will do the same (not shown). It is seen that the average penetration

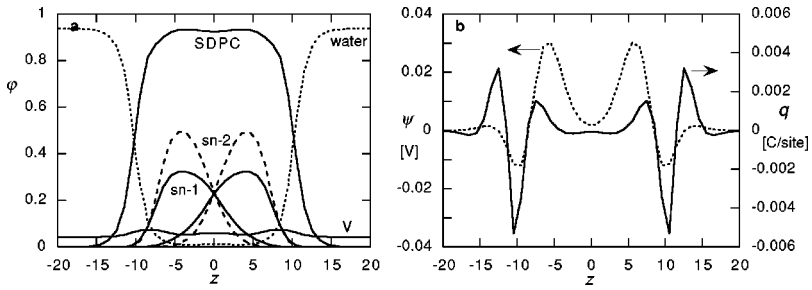

FIG. 6. (a) Selection of distribution functions of the SDPC bilayer system. The following distributions are shown as indicated: the overall profile, the distribution of water and free volume as well as the contributions of the *sn*-1 and *sn*-2 chains (of each monolayer), (b) the electrostatic potential profile (left ordinate) and the overall charge distribution (right ordinate).

of the *sn*-1 chain into the opposite bilayer saturates for negative χ_{PW}. However, one should realize that the membrane thickness decreases with increasing hydrophilicity of the P units and therefore the relative penetration depth still increases. The membrane should thus be classified as (partly) interdigitated. The *sn*-2 chain, however, remains on average on the positive side of the bilayer. This illustrates again the dramatic effect of unsaturation. Unsaturation strongly suppresses membrane interdigitation.

In Fig. 5(c) the difference in the order parameter at the position $s=10$ of the saturated acyl and the unsaturated chain $\Delta S_{CH}=S_{CH}(s_{sn_1}=10)-S_{CH}(s_{sn_2}=10)$ is given again as a function of the hydrophilicity of the P group. It is seen that the relative dip in the order parameter decreases with increasing hydrophilicity of the head group. The reason for this is that the overall value of the order parameter profile is reduced when the membrane thickness is reduced. The absolute value of the order parameter at the dip is not much affected by this. This explains the trend shown in Fig. 5(c).

Finally, in Fig. 5(d) the difference in average position of the choline group and that of the phosphate group is plotted, $\langle z\rangle_{N\text{-}P}\equiv\langle z\rangle_N-\langle z\rangle_P$ again as a function of the value of the χ parameter used for the phosphate-water interaction. In the present model this value tends to be negative, which means that it is the phosphate group that is positioned more on the outside rather than the choline group. It was shown before that it is possible to change the head-group orientation by the addition of a charged additive [22]. The orientation of the head-group may also depend on the choices made in the way the charge is distributed in the choline group. In the SCF model the positive charge is placed on the N atom, whereas in the MD results discussed below the charge is more evenly distributed over the choline group.

The dashed lines in Fig. 5 correspond to the classical approach of equal volumes for the CH_2 and CH_3 groups. The most dramatic effect of this choice is that the saturated chain end is at negative coordinates for all values of the P-water interaction. This means that the *sn*-1 chain is crossing the center of the bilayer for all these cases. From this it is clear that, in order to obtain noninterdigitated bilayers, it is essential to choose the proper intrinsic volume of the acyl end group. Indeed, when the *sn*-1 chain is interdigitating the opposite side of the bilayer [cf. Fig. 5(b)] the order along the chain is higher [cf. Fig. 5(c)], the area per molecule tends to be lower [cf. Fig. 5(a)], i.e., the membrane is a bit thicker, and the orientation of the head group is even more flat [cf. Fig. 5(d)].

It is of interest to compare these results for the membrane characteristics found for $\chi_{P\text{-}H_2O}=0.5$ with the results presented in Figs. 3 and 4. This comparison illustrates the effect of ignoring the disparities between interactions of CH_2 and CH_3 groups with their surroundings. In Fig. 5 the values for the bilayer when all parameters are given by Table I are given by the symbols. Indeed inspection of the result of Fig. 5 shows that the membrane characteristics for the bilayer with $\chi_{P\text{-}H_2O}=0.5$ are not very strong functions of the parameters $\chi_{CH_3\text{-}CH_2}$, $\chi_{CH_3\text{-}O}$ and $\chi_{CH_3\text{-}V}$. Nevertheless, the small differences remain worth discussing. In Fig. 5(b) it is seen that dismissing the enthalpic effects allows the chain ends to be positioned at lower coordinates, i.e., the chains are penetrating deeper into the other side of the bilayer. At the same time the area per molecule tends to be a bit higher [cf. Fig. 5(a)] when the chain ends can penetrate deeper in the bilayer. This can be explained by results of Fig. 5(c) where it is shown that the order in the chains tends to be higher when there is no enthalpic difference between contacts of CH_2 and CH_3 groups with other segments. The orientation of the head group is not much affected of course by dismissing the enthalpic differences between the CH_2 and CH_3 groups [cf Fig. 5(d)].

Before moving on to discuss the molecular dynamics simulation results, a selection of the properties of the SDPC, 18:0/22:6 PC, bilayer system is presented (again using the standard parameter set). The SDPC lipids are composed of two acyl chains of which the *sn*-1 chain is again the fully saturated C18 chain. The *sn*-2 chain is 22 carbons long and has 6 unsaturated bonds: C3—C4=C5—C6, C6—C7=C8—C9, C9—C10=C11—C12, C12—C13=C14—C15, C15—C16=C17—C18, C18—C19=C20—C21. The equilibrated membrane, i.e., the membrane which is free of tension, differs in several aspects from the SOPC membrane. The area per molecule for the SDPC molecules is predicted to be $a_o=12.66\ell^2$. This is significantly larger than that of the DOPC membranes. The phosphorus-phosphorus distance (membrane thickness) is determined to be $d_{PP}=19.025\ell$. In Fig. 6 some overall characteristics are presented. The overall membrane density profile, the water density profile, and the free volume distribution are very similar as in the DOPC layers as shown in Fig. 6(a). The dip in the center of the bilayer is more pronounced than in the SOPC case. The distribution of the *sn*-2 chain differs significantly from that of the *sn*-1 chain. Interestingly, the *sn*-2 chain, which is four carbon segments longer than the *sn*-1 chain does not penetrate as far into the opposite monolayer as the *sn*-1 chain.

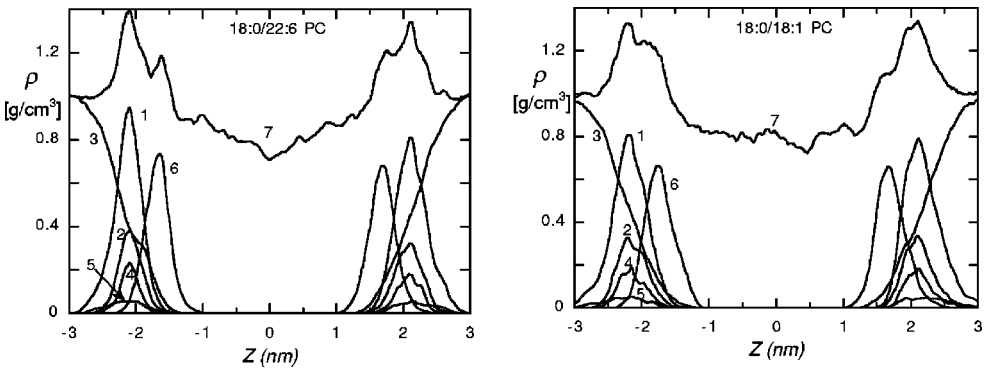

FIG. 7. Mass density distributions for selected groups of atoms in hydrated bilayers of 18:0/18:1 PC and 18:0/22:6 PC along the bilayer normal: PC head groups (1), four oxygen atoms of phosphate PO_4 groups (2), water (3), phosphorus atoms (4), nitrogen atoms (5), atoms of glycerol and groups O—C═O (6), all the system—the head atoms, glycerol, atoms of lipid hydrocarbon chains, and water (7). The MD simulation systems were 48 times 2 lipids per cell, 24 H_2O molecules per lipid, all together there were 20 352 (SOPC) and 20 544 (SDPC) atoms. Mean cross-sectional areas per lipid molecule were 0.6134 and 0.6624 nm^2. The MD trajectories of 1018 ps were computed at $T=303$ K. Zero point ($z=0$) is the center of the bilayer: it was calculated during the MD simulations as the middle point between the centers of P-N vectors of the two monolayers (the center of P-N vector is the middle of P-N distance).

However, the difference is not large and therefore it is possible for the *sn*-1 chain to behave rather similar in the DOPC layer and in the SOPC membranes (cf. Fig. 4).

In Fig. 6(b) the electrostatic potential profile as well as the overall charge profile through the cross section of the SDPC bilayer are presented. The corresponding curves for the SOPC layers is given in Fig. 3(b). Again the overall characteristics are rather similar. This is not too surprising because the electrostatic effects are generated by the zwitter-ionic head-group conformations. These are not so much affected by the tails. Close inspection, however, reveals that the absolute values of the charge and the potential profiles differ somewhat, the absolute values are the largest in the SDPC case. From the increase in area per lipid molecule an opposite trend could have been expected. Apparently, more freedom for the head-group orientation allows for effectively fewer head groups to lay parallel to the membrane surface. This implies that packing effects do not determine the level of out-of-plane orientation of the head groups.

MOLECULAR DYNAMICS SIMULATIONS

The detailed description of the MD approach, the mathematical model used, the PC bilayer simulation box and the force field characteristics were presented in our previous paper [2]. The principle of the MD method is as follows. In the MD process, the equations of motion of all the atoms of the molecular system are solved. MD algorithm consists of the creation of an initial configuration and then the simulation procedure: a new configuration is generated by solving the equation of motions, with time step Δt, and so on. After k steps one can obtain time-dependent properties of the system (time dependences and time-averaged quantities), see, e.g., Refs. [39,40]. Our simulation boxes for the bilayers consisted of 48 lipid molecules per layer and 24 H_2O molecules per lipid (in all, 96 PC molecules and 2304 water molecules in each bilayer). Each lipid molecule contains the saturated 18:0 chain and unsaturated 18:1 (in the first bilayer) or 22:6 (in the second one) chain. The structure of lipid molecules—the two hydrocarbon tails, the glycerol section, the head group of PC—were treated in accordance with their real chemical structure, all hydrogen atoms were included explicitly in the calculations. A total number of atoms in the simulation box was 20 352 for 18:0/18:1 PC bilayer and 20 544 for 18:0/22:6 PC bilayer. The initial structures of the bilayers were crystallike ordered structures [2].

The potential energy U of a bilayer was calculated as sum of the bond-stretching energy, the angle-bending energy, the torsion energy, the out-of-plane energy (for the double bonds and the carbonyl groups), the van der Waals energy and the electrostatic energy. Equations of motion were integrated by using the ''velocity Verlet'' algorithm [39,40] with the simulation time step of 1 fs (10^{-15} sec). Periodic boundary conditions in the three directions were used. The two unsaturated bilayer systems were coupled to an external temperature bath of 303 K and pressure bath ($P_x, P_y, P_z = 1$ atm). MD simulations were performed using collisional dynamics [2]. The trajectories of 1018 ps were calculated. The average areas per molecule during the simulations were 0.6134 nm^2 for 18:0/18:1 PC bilayer and 0.6624 nm^2 18:0/22:6 PC bilayer.

MD results for SOPC and SDPC bilayers

Mass density profiles along the bilayer normal for the head groups, oxygens of phosphate groups, water molecules, phosphorus and nitrogens atoms, glycerol and all the system, for a hydrated unsaturated 18:0/18:1 PC and polyunsaturated 18:0/22:6 PC bilayers are shown in Fig. 7. To calculate these profiles, the total mass of the atoms per slice of 0.01 nm along the normal was calculated. The profiles were time averaged over a period of 1018 ps of the MD simulation. It is seen that the water molecules penetrate into the bilayers up to the region of C═O groups of the acyls. The mass density profiles of both bilayer systems have two peaks (the locations of the phosphate groups) and a minimum (or plateau) near the center of the bilayers. The minimum of polyunsaturated bilayer is deeper than that for monounsaturated one. This last finding is in line with the SCF results discussed

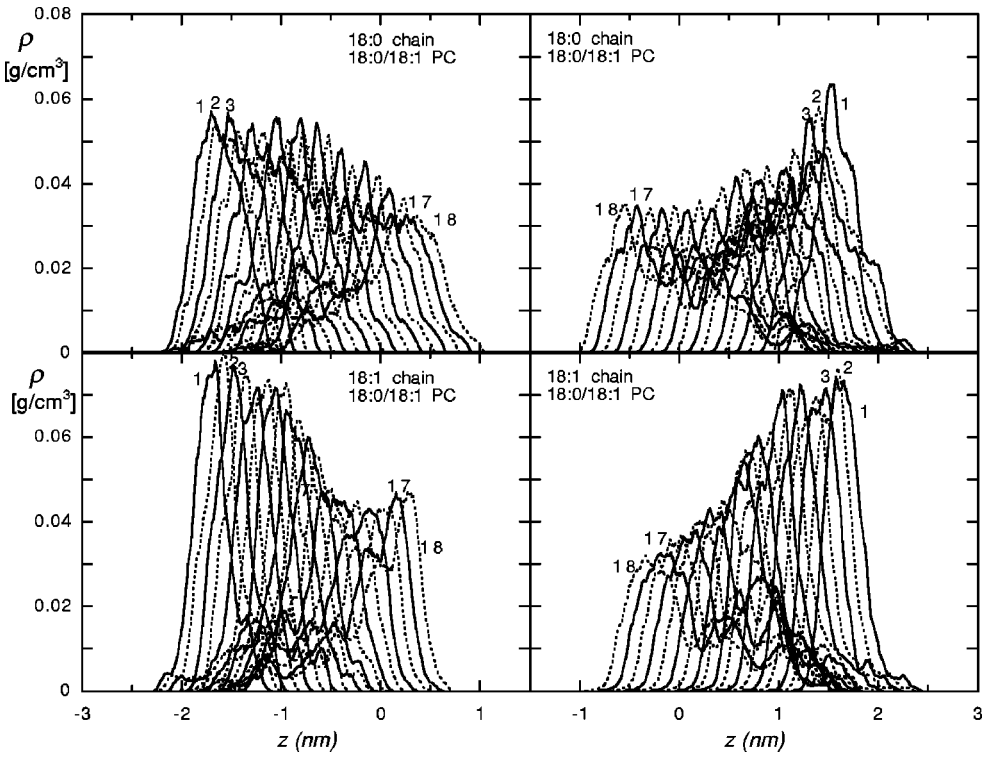

FIG. 8. Mass density profiles along the normal for each carbon atoms of (left) the first monolayer and (right) the second monolayer saturated and monounsaturated chains of the 18:0/18:1 PC bilayer; the MD computer simulations, $t=1018$ ps, $T=303$ K. The carbon atom of C═O group is carbon number 1. Some segment ranking numbers are indicated. Profiles are drawn alternating as dashed and as solid lines.

above. The position of the bilayer center ($z=0$) was calculated during the simulations as the middle point between the centers of P—N vectors of the two monolayers (where the center of P—N vector is the middle of P—N distance). The average distance between P—N vectors along the normal is 4.39 nm for 18:0/18:1 PC and 4.28 nm for 18:0/22:6 PC bilayer. The average phosphorus-phosphorus distances d_{PP} are 4.27 and 4.18 nm, respectively. Again there are several similarities between the MD and SCF results. For example, it is seen that the distribution of the N is wider than that of the P, the distribution of the head group and glycerol unit overlaps weakly and there are no head groups found in the core of the bilayer.

The result is qualitatively in line with experimental data and the data of different computer simulations of saturated and unsaturated lipid bilayers. Thus, according to x-ray diffraction studies, d_{PP} is equal to 4.05 nm (± 0.1 nm) for 18:0/18:0 PC bilayer at $T=333$ K [41] and $d_{PP}=4.04$ nm for 18:1/18:1 PC bilayer [33]. It was obtained in MD simulations for 16:0/18:2 PC bilayer at $T=321$ K (area per molecule$=0.7056$ nm^2) that $d_{\mathrm{PP}}=4.16$ nm [42] and for 18:1/18:1 PC bilayer at $T=296$ K (area per molecule$=0.593$ nm^2) that $d_{\mathrm{PP}}=4.25$ nm [43].

Figures 8 and 9 show the carbon atom distributions of SOPC and SDPC bilayers calculated by the MD investigations. In these graphs both monolayers of the bilayer systems are shown. From the difference between the two monolayers, one can evaluate the success of the averaging procedure: in principle both monolayers should be identical. It should be mentioned that some of the distributions are polymodal: the mass density picture is rather complex. On the whole, the profiles of the carbons near the chain ends are wider than those situated near the glycerol part. An interesting situation was observed for the 18:0/18:1 PC bilayer: the z positions of the end carbon's centers (carbons number 18) of sn-1 chains of the first and the second monolayers overlap, $z=0.10$ nm for the first (left) monolayer sn-1 carbon and $z=-0.07$ nm for the second (right) monolayer sn-1 carbon. The z-positions of the end carbon's centers of sn-2 chains of the first and the second monolayers are -0.09 nm and 0.15 nm, so they are separated. All the end carbon's z positions of the opposite monolayers of 18:0/22:6 PC bilayer are separated as well.

The influence of the double bonds may again be discussed by considering the peak value and the peak position of the segment distributions. Of course the noise in the MD simulations does not make this operation easy. Nevertheless, the curve $\rho^{max}(z^{max})$ is to a good approximation a straight line for the sn-1 chain, both for the SOPC and the DOPC case. In the SCF result a curved line was found. This indicates that the tails in the SCF model randomize near the chain ends more than in the MD simulations. In line with the SCF result for the SOPC case presented above, there is a very pronounced break in the $\rho^{max}(z^{max})$ curve near $s=10$ in the sn-2 tail of the SOPC bilayer. In the DOPC bilayer, the sn-2 chain has six cis double bonds positioned on regular positions along the chain. As a result the $\rho^{max}(z^{max})$ curve for the sn-2 chain of DOPC is again almost a straight line, albeit

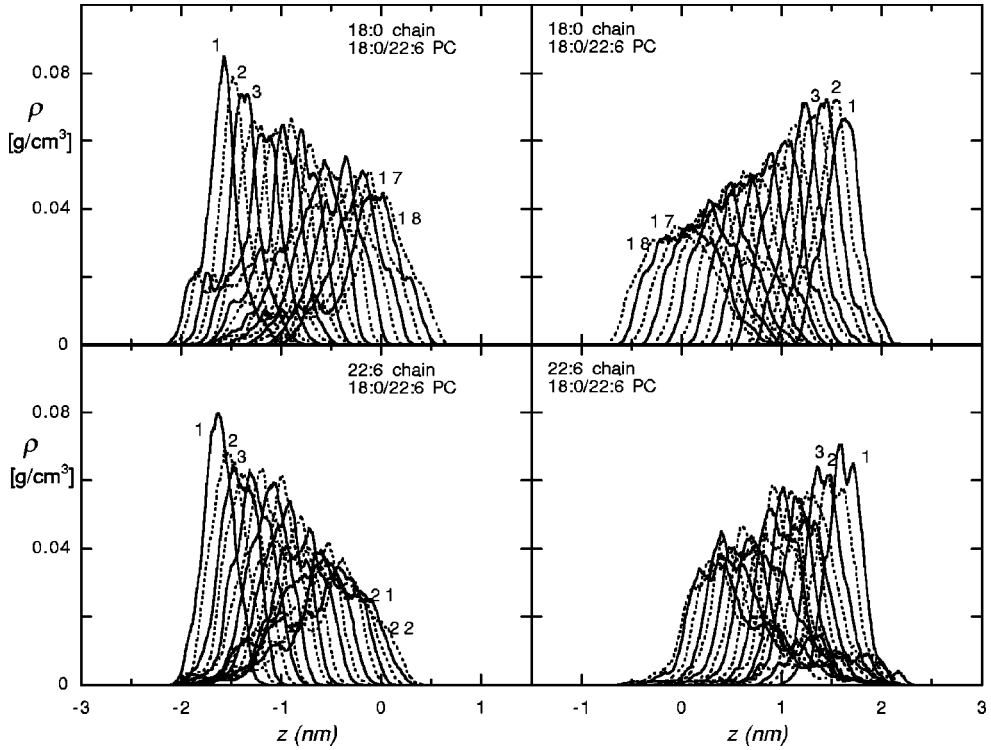

FIG. 9. Mass density profiles along the normal for each carbon atoms of (left) the first monolayer and (right) the second monolayer saturated and polyunsaturated chains of the 18:0/22:6 PC bilayer; the MD computer simulations, $t=1018$ ps, $T=303$ K. The carbon atom of C═O group is carbon number 1. Some segment ranking numbers are indicated. Profiles are drawn alternating as dashed and as solid lines.

that the slope is high, i.e. ρ^{max} drops very quickly with z^{max} (with increasing s).

The mass density distributions of the glycerol backbone carbons (not shown) are monomodal and the narrowest as compared with the distributions of Figs. 8 and 9. This is in good agreement with the SCF results where the distribution of the glycerol backbone units were found to be the narrowest in the whole molecule.

The mean angles of the P—N vectors with respect to the bilayer surfaces were calculated. These were 15.5° (18:0/18:1 PC) and 12.8° (18:0/22:6 PC) in the MD simulations. These findings are in line with the data of experiment and different computer simulations as mentioned (and referenced) above. In the SCF results also a small angle of the head group with respect to the bilayer surface was reported, albeit that a small negative value was found.

DISCUSSION AND OUTLOOK

All-atom MD simulations give extremely detailed and rich information on the lipid bilayer systems, much more detailed as could be discussed in the MD results for SOPC and SDPC bilayers section (see also Ref. [2]). This comes at a prize: the MD procedure is very demanding on the computer power. The SCF technique on the other hand is computationally very inexpensive. It was shown that this quick technique already presents a detailed picture of the bilayer system. Comparison of MD with the SCF results shows that the SCF results are also reasonably reliable. One clear advantage is that the results are noise-free, which facilitates the discussion of the predictions. The accuracy of the SCF approach should in principle be considered as a surprise, especially considering the very serious approximations made in the SCF technique. The most severe approximation is that the system of many chains is reduced to a single chain in an external field. However, detailed Monte Carlo analysis of single chains of the type similar to the acyl chains in the lipids [45,44] (for a review, see also Ref. [2]) revealed that the intramolecular properties of the single chains can, in first approximation, be compared to the conformational properties of the chains packed in the bilayer. This shows that the tail properties in the bilayer are in first order following the intramolecular characteristics and that in second order these characteristics are modified by the surrounding lipids. This result may be related to the success of SCF modeling. The single-chain characteristics survive in the bilayer and thus the SCF technique can do a good job describing the bilayer system.

More sensitive measure of the success of the SCF method is the prediction of the area per molecule of the equilibrated bilayer. Indeed, the SCF results follow the MD prediction as well as the experimental facts semiquantitatively. To appreciate this result, it is necessary to recall that in order to predict the area per molecule one should compute the membrane tension as a function of the area per molecule. Apparently, the SCF technique is doing a good job in predicting this thermodynamic property. In the SCF results there is still the

length ℓ which may be used to translate the lattice results to real coordinates. If a value of $\ell = 0.23$ nm is used, reasonable quantitative agreement is found both with respect to the area per molecule and the thickness of both bilayers.

Lipid unsaturation is an important fact in biological membranes [2]. Above it was argued that unsaturation helps the bilayer to remain in the fluid state. The unsaturation along the chain effectively reduces the (effective) length of the chain. It is for this reason that, especially when the chains have multiple double bonds, the tails have more C atoms than the saturated chains in the lipids. Further, it was argued that lipid unsaturation may be used in bilayer systems to counteract the interdigitation of lipids into the opposite monolayer. The more lipid chains cross the midplane of the bilayer the stronger is the coupling between the two leaflets. Of course some coupling will be necessary. The use of unsaturated lipids in the bilayer may help to regulate this property.

The advantage of doing SCF calculations is that, once the parameters needed in the SCF modeling are known, other characteristics are within reach. It is recently shown that it is possible to find the Helfrich parameters from the analysis of curved bilayers (vesicles) [25]. There are two important parameters, one parameter expresses the resistance against bending and the other one is associated with the formation of saddle shaped geometries. The first one is of importance for understanding the undulation force between bilayers, the other one determines the topology of the membrane system. In other words, if these parameters are known, one can obtain some insight into the phase behavior of the lipids. The route to obtain these parameters for lipid systems is in principle open.

It is further possible to model lipid mixtures in the SCF approach. These systems are of course important in the biological context. It will then be more clear what the true role of lipid unsaturation is. It is speculated on in the literature that the unsaturated lipids have a function as boundary lipids around proteins (for details, see Ref. [2]). These and other aspects will be the subject of future research.

SUMMARY

The bilayer properties of 1-stearoyl-2-oleoyl-*sn*-glycero-3-phosphatidylcholine (18:0/18:1 PC, SOPC) and 1-stearoyl-2-docosahexaenoyl-*sn*-glycero-3-phosphatidylcholine (18:0/22:6, SDPC) were investigated by a molecular realistic self-consistent-field (SCF) theory. The molecular details were represented as accurate as presently possible and the results were compared to an all-atom molecular dynamics simulation. The MD simulations, which are more detailed and better validated, are used to judge the performance of the SCF theory. The general findings are that the SCF approach, which is 10^4 to 10^5 times faster than the MD technique, captures the main results for this system at least semiquantitatively and almost quantitatively.

Acyl unsaturation has a strong effect on the chain ordering and the level of chain interdigitation. It is well known that volume of a CH_3 group is to a good approximation twice that of a CH_2 group. This volume disparity is significant as it strongly opposes interdigitation. Differences in (enthalpic) interactions between CH_3 and CH_2 groups with other molecules are secondary in this respect. The water molecules will not enter the bilayer beyond the glycerol backbone units. Free volume is almost evenly distributed through the bilayer. Only small increases of free volume levels are found in the glycerol backbone region and in the membrane center. The parameters needed in the SCF approach are now reasonably validated by the MD results. The availability of reliable parameters for a SCF model gives an excellent perspective for future SCF investigations of other membrane properties such as the mechanical parameters of the bilayers. These last parameters are important to understand the phase behavior of lipids. A more detailed analysis of the hydrophobic region of the bilayers is discussed in the previous paper of this issue [2].

ACKNOWLEDGMENTS

This work was partially supported by the NWO Dutch-Russian program for polyelectrolytes in complex fluids and the Russian Foundation for Basic Research, Grant Nos. 00-03-33181 and 01-04-48050.

[1] A. L. Lehninger, D. L. Nelson, and M. M. Cox, *Principles of Biochemistry* (Worth, New York, 1993).
[2] A. L. Rabinovich, P. O. Ripatti, N. K. Balabaev, and F. A. M. Leermakers, preceding paper, Phys. Rev. E **67**, 011909 (2003). Molecular dynamics simulations of hydrated unsaturated lipid bilayers in the liquid-crystal phase and comparison to self-consistent-field modeling.
[3] R.W. Pastor, Curr. Opin. Struct. Biol. **4**, 486 (1994).
[4] K. V. Damodaran and K. M. Merz, Jr., in *Reviews in Computational Chemistry*, edited by K. B. Lipkowitz, and D. B. Boyd, (VCH, New Yok, 1994), Vol. 5, pp. 269–298.
[5] D.J. Tobias, K. Tu, and M.L. Klein, Curr. Opin. Colloid Interface Sci. **2**, 15 (1997).
[6] D.P. Tieleman, S.J. Marrink, and H.J.C. Berendsen, Biochim. Biophys. Acta **1331**, 235 (1997).
[7] R.S. Cantor, Biophys. J. **76**, 2625 (1999).
[8] S. Marcelja, Biochim. Biophys. Acta **367**, 165 (1974).
[9] D.W.R. Gruen, J. Phys. Chem. **89**, 146 (1985).
[10] D.W.R. Gruen, Biochim. Biophys. Acta **595**, 161 (1980).
[11] D.W.R. Gruen and D.A. Haydon, Biophys. J. **33**, 167 (1981).
[12] K.A. Dill, J. Naghizadeh, and J.A. Marqusee, Annu. Rev. Phys. Chem. **39**, 425 (1988).
[13] A. Ben-Shaul and W. M. Gelbart, in *Micelles, Monolayers, Microemulsions and Membranes*, edited by W. M. Gelbart, A. Ben-Shaul, and D. Roux (Springer, New York, 1994), pp. 1–104.
[14] I. Szleifer, A. Ben-Shaul, and W.M. Gelbart, J. Chem. Phys. **85**, 5345 (1986).
[15] R.S. Cantor and K.A. Dill, Langmuir **2**, 331 (1986).
[16] F.A.M. Leermakers, J.M.H.M. Scheutjens, and J. Lyklema, Biophys. Chem. **18**, 353 (1983).
[17] P. van der Ploeg and H.J.C. Berendsen, J. Chem. Phys. **76**, 3271 (1982).

[18] P. van der Ploeg and H.J.C. Berendsen, Mol. Phys. **49**, 233 (1983).
[19] F.A.M. Leermakers and J.M.H.M. Scheutjens, J. Chem. Phys. **89**, 3264 (1988).
[20] L.A. Meijer, F.A.M. Leermakers, and J. Lyklema, Recl. Trav. Chim. Pays-Bas. **113**, 167 (1994).
[21] F.A.M. Leermakers and J.M.H.M. Scheutjens, J. Chem. Phys. **89**, 6912 (1988).
[22] L.A. Meijer, F.A.M. Leermakers, and J. Lyklema, J. Phys. Chem. **99**, 17282 (1995).
[23] F.A.M. Leermakers and J.M.H.M. Scheutjens, J. Chem. Phys. **93**, 7417 (1989).
[24] S.M. Oversteegen and E.M. Blokhuis, J. Chem. Phys. **112**, 2980 (1999).
[25] S.M. Oversteegen and F.A.M. Leermakers, Phys. Rev. E **62**, 8453 (2000).
[26] S.M. Oversteegen, P.A. Barneveld, J. van Male, F.A.M. Leermakers, and J. Lyklema, Phys. Chem. Chem. Phys. **1**, 4987 (1999).
[27] S.J. Suresh and V.M. Naik, Langmuir **12**, 6151 (1996).
[28] L.A. Meijer, F.A.M. Leermakers, and J. Lyklema, J. Chem. Phys. **110**, 6560 (1999).
[29] N.A.M. Besseling and J.M.H.M. Scheutjens, J. Phys. Chem. **98**, 11610 (1993).
[30] B. Smit, P.A.J. Hilbers, K. Esselink, L.A.M. Rupert, N.M. van Os, and A.G. Schlijper, J. Chem. Phys. **95**, 6361 (1991).
[31] F.A.M. Leermakers and M.A. Cohen Stuart, Phys. Rev. Lett. **76**, 82 (1996).
[32] B. Smit, S. Karaborni, and J.I. Siepmann, J. Chem. Phys. **102**, 2126 (1995).
[33] M.C. Wiener and S.H. White, Biophys. J. **61**, 434 (1992).
[34] H. Akitsu and T. Nagamori, Biochemistry **30**, 4510 (1991).
[35] J. Seelig, P.M. MacDonald, and P.G. Scherer, Biochemistry **26**, 7535 (1987).
[36] H. Hauser, I. Pascher, R.H. Pearson, and S. Sundell, Biochim. Biophys. Acta **650**, 450 (1987).
[37] G. Büldt, H.U. Gally, A. Seelig, and G. Zaccai, J. Mol. Biol. **134**, 673 (1979).
[38] R.M. Peitzsch, M. Eisenberg, K.A. Sharp, and S. McLaughlin, Biophys. J. **68**, 729 (1995).
[39] R. J. Sadus, *Molecular Simulations of Fluids. Theory, Algorithms and Object-Orientation* (Elsevier, Amsterdam, 1999).
[40] M. P. Allen and D. J. Tildesley, *Computer Simulation of Liquids* (Clarendon Press, Oxford, 1987).
[41] B.A. Lewis and D.M. Engelman, J. Mol. Biol. **166**, 211 (1983).
[42] M.T. Hyvönen, T.T. Rantala, and M. Ala-Korpela, Biophys. J. **73**, 2907 (1997).
[43] S.E. Feller, D. Yin, R.W. Pastor, and A.D. Mackerell, Jr., Biophys. J. **73**, 2269 (1997).
[44] A.L. Rabinovich and P.O. Ripatti, Biofizika **45**, 823 (2000) [Biophysics (Engl. Transl.) **45**, 797 (2000)].
[45] A.L. Rabinovich and P.O. Ripatti, Biofizika **42**, 874 (1997) [Biophysics (Engl. Transl.) **42**, 879 (1997)].